

Lattice Spacing Effect on Scan Loss for Bat-Wing Phased Array Antennas

Thinh Q. Ho*, Charles A. Hewett, Lilton N. Hunt
SSCSD 2825, San Diego, CA 92152
Thomas G. Ready
NAVSEA PMS500, Washington, DC 20376
Raj Mittra
RM Associates, State College, PA 16803

I. Introduction

Phased array antennas are becoming increasingly more important in communications and radar applications [1]. In general, these arrays are designed to produce narrow directional beams with hemispherical coverage. From the system design perspective, a phased array antenna must be implemented using multiple co-located antenna panels to meet the gain requirement over the entire scan volume. In order to accomplish this technical objective, and yet at the same time minimize the total element count, a phased array system must be designed with an acceptable scan loss. Within this context, positive link margin is always available in the boresight direction; the challenge is to satisfy the above requirement at the crossover point between antenna panels, or at the edge of coverage. In this paper, a trade-off study between directivity and scan loss with respect to element spacing for a 64-element bat-wing phased array with a triangular lattice is carried out using a newly developed parallelized CFDTD code. Data on scan loss performance as a function of lattice spacing is presented.

II. Details of Array Geometry

This investigation addresses three similar antenna arrays, distinguishable by the spacing between their radiators (0.5λ , 0.65λ , and 0.8λ at the operating frequency of 15 GHz). The phased array antennas are made up of orthogonal bat-wing pairs arranged on a triangular lattice. The orthogonal radiators form a cross where one dipole is positioned slightly above the other. The elements are printed on 8 mil thick substrates with a dielectric constant of 1.07 and positioned perpendicular to a 3.53×4.08 inch ground plane. The arms of the dipole are also tilted toward the ground plane. The distance from the center of the lowest tilted arm pair to the ground plane is 162 mils (0.205λ). The bat wing arms are tilted 30° with respect to the ground plane. Figure 1 shows the layout of the phased array antenna.

III. Numerical Modeling

Computational electromagnetic modeling is very important to the development of array antennas due to the high cost of fabricating and testing phased arrays. In general, computer simulations can provide accurate results in less time, at lower cost and with reduced risk. The newly developed Conformal Finite Difference Time Domain (CFDTD) solver has been designed for this purpose [2]. The CFDTD method has several advantages for phased array antenna modeling. First, the method can handle arbitrary geometries and material media, *i.e.*, no restrictions are placed on the shape and composition of the structure to be analyzed. The method also rigorously accounts for element interactions, as well as dielectric, parasitic and edge effects. The antennas modeled contain 64 bat-wing elements positioned upright with respect to a finite ground plane. The array is modeled as a finite structure and its elements are arranged in a triangular lattice configuration. Numerically, this requires a discretization of the computational domain into a large number of cells in order to achieve accurate results. The CFDTD algorithm utilizes a versatile non-uniform mesh in the problem space, minimizing the computer memory

Report Documentation Page				Form Approved OMB No. 0704-0188	
Public reporting burden for the collection of information is estimated to average 1 hour per response, including the time for reviewing instructions, searching existing data sources, gathering and maintaining the data needed, and completing and reviewing the collection of information. Send comments regarding this burden estimate or any other aspect of this collection of information, including suggestions for reducing this burden, to Washington Headquarters Services, Directorate for Information Operations and Reports, 1215 Jefferson Davis Highway, Suite 1204, Arlington VA 22202-4302. Respondents should be aware that notwithstanding any other provision of law, no person shall be subject to a penalty for failing to comply with a collection of information if it does not display a currently valid OMB control number.					
1. REPORT DATE 01 JAN 2005		2. REPORT TYPE N/A		3. DATES COVERED -	
4. TITLE AND SUBTITLE Lattice Spacing Effect on Scan Loss for Bat-Wing Phased Array Antennas				5a. CONTRACT NUMBER	
				5b. GRANT NUMBER	
				5c. PROGRAM ELEMENT NUMBER	
6. AUTHOR(S)				5d. PROJECT NUMBER	
				5e. TASK NUMBER	
				5f. WORK UNIT NUMBER	
7. PERFORMING ORGANIZATION NAME(S) AND ADDRESS(ES) SSCSD 2825, San Diego, CA 92152				8. PERFORMING ORGANIZATION REPORT NUMBER	
9. SPONSORING/MONITORING AGENCY NAME(S) AND ADDRESS(ES)				10. SPONSOR/MONITOR'S ACRONYM(S)	
				11. SPONSOR/MONITOR'S REPORT NUMBER(S)	
12. DISTRIBUTION/AVAILABILITY STATEMENT Approved for public release, distribution unlimited					
13. SUPPLEMENTARY NOTES See also ADM001846, Applied Computational Electromagnetics Society 2005 Journal, Newsletter, and Conference., The original document contains color images.					
14. ABSTRACT					
15. SUBJECT TERMS					
16. SECURITY CLASSIFICATION OF:			17. LIMITATION OF ABSTRACT UU	18. NUMBER OF PAGES 4	19a. NAME OF RESPONSIBLE PERSON
a. REPORT unclassified	b. ABSTRACT unclassified	c. THIS PAGE unclassified			

requirements for large array models, whose elements generally have a complex geometry. Finer gridding is applied in the vicinity of the radiating elements and the ground plane edges, while coarse gridding is used elsewhere. The computational domains of the antenna models were terminated with perfectly matched layer absorbing boundary conditions [3]. The radiators were excited by placing an electric field directly across the gap of the two segments of each bat-wing element. A 90° phase difference is introduced between the orthogonal pairs in order to achieve circular polarization. The main beam of each array was scanned off boresight to four different scan angles: 15° , 30° , 45° , and 60° . The progressive phase delays necessary to steer the beam away from boresight were applied directly to the source of each element.

IV. Results and Discussion

Table 1 displays the directivity values at boresight over the frequency range 14.4 GHz to 15.4 GHz for each of the element spacings. The direction of maximum radiation was steered off boresight in the $\phi = 90^\circ$ plane to four elevation angles, $\theta = 15^\circ$, 30° , 45° , and 60° . Radiation patterns for the array with 0.65λ element separation are shown in Figure 2. The boresight pattern shows a directivity of 24.56 dB and a beamwidth of 9.6° at 15 GHz. There are five sidelobes ranging from 13 to 37 dB below the main lobe. When the element spacing is reduced to 0.5λ , the boresight directivity drops to 22.44 dB; it rises to 26.14 dB when the element spacing is increased to 0.8λ . As the main beam is scanned off boresight, the antenna radiation becomes less directive. At a scan angle of 30° , the maximum radiation intensity decreases by 0.34 dB, 0.43 dB, and 2.0 dB for 0.5λ , 0.65λ , and 0.8λ spacing, respectively. The first sidelobe of each array remains at approximately -13 dB relative to the peak. When the beam is scanned to 45° the drops in directivity relative to the boresight values are 0.94 dB, 1.33 dB, and 4.84 dB. The first sidelobe peak increases to 12.5 dB below that of the main beam for all spacings. At 60° the drop offs are 2.1 and 3.7dB for 0.5λ and 0.65λ spacing. In the case of the 0.8λ element spaced array, the major lobe at $\phi = 90^\circ$, $\theta = 60^\circ$ has a directivity of 19.0 dB. However, this is not the direction of maximum radiation. In fact, there are grating lobes in the $\phi = 208^\circ$ & 332° planes that correspond to the directions of maximum radiation, and the directivities of these grating lobes equal 19.9 dB.

Figure 3 shows the relationship between the scan angle and the directivity for three different element spacings: 0.5λ , 0.65λ and 0.8λ . We note that the directivity at boresight is greater for arrays with a large separation between the radiating elements. Recall that the difference in directivity between the 0.8λ and 0.5λ element separation is 3.7 dB. However, the greater gain at boresight comes with a sharp rate of decline in directivity as the beam is scanned away from boresight. As shown in Figure 3, the directivity of the 0.8λ array declines to a value less than that of the 0.65λ array when the main beam is scanned to 30° . When the beam is scanned to 45° , the directivity declines to a value less than that of the 0.5λ array. At 60° , the radiation characteristics of this array become unacceptable since grating lobes in non-principal planes have overtaken the scanned lobe. The analysis of the 0.5λ array shows that, from boresight to 60° , only 2dB of directivity is lost compared to 3.7 and 6.2 dB for the 0.65λ and 0.8λ case array spacings, respectively. The key point about this study is that when designing phased arrays to provide full hemispherical coverage, a choice must be made between a large boresight gain with a steep scan roll-off or a much lower boresight gain with a mild scan roll-off. For applications with strict crossover point requirements, it is more desirable to maintain a constant gain characteristic. Currently, antenna designers use $\cos^n(\theta)$ as a rule of thumb to predict the gain roll-off. This work has shown that care must be taken when applying this guideline.

Acknowledgements

This work was part of the Integrated Topside Design VIPER Tool Set Development funded by NAVSEA PMS-500.

References

- [1] R. J. Mailloux, *Phased Array Antenna Handbook*, Artech, 1994.
- [2] W. Yu and R. Mittra, *Conformal Finite Difference Time Domain Solver*, New York: Artech House, 2004
- [3] A. Taflov and S. C. Hagness, *Computational Electrodynamics: The Finite-Difference Time Domain Method*, 2nd Edition, New York: Artech House, 2000.

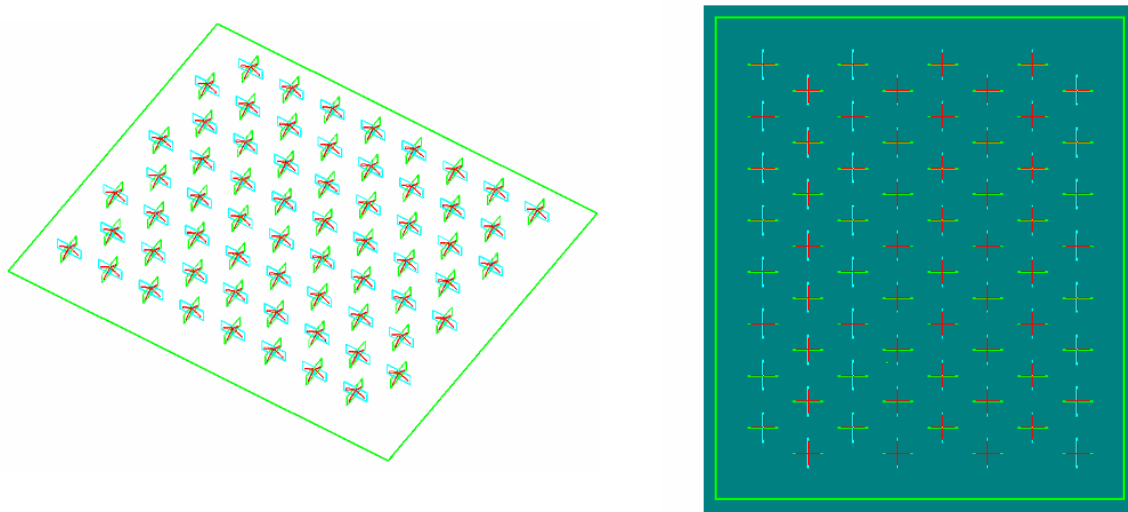


Figure 1. Geometry of the 64-element bat-wing array.

Table 1. Boresight directivity (dB) vs. frequency.

Frequency	0.5λ Spacing	0.65λ Spacing	0.8λ Spacing
14.4 GHz	22.18	24.33	25.93
14.6 GHz	22.27	24.41	26.01
14.8 GHz	22.36	24.48	26.10
15.0 GHz	22.44	24.56	26.14
15.2 GHz	22.52	24.63	26.20
15.4 GHz	22.60	24.69	26.27

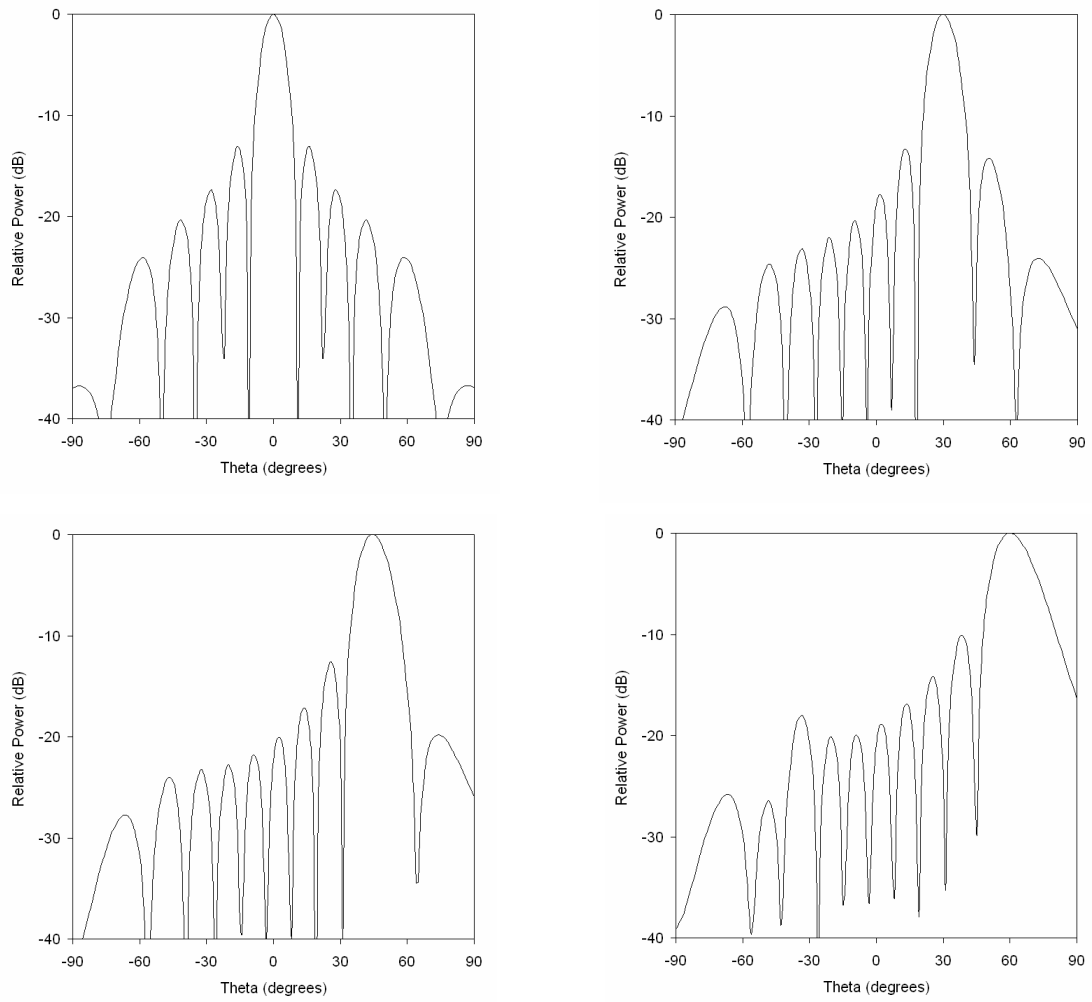


Figure 2. Radiation patterns at $\theta = 0^\circ$, 30° , 45° , & 60° scan angles for a triangular lattice array with 0.65λ element separation.

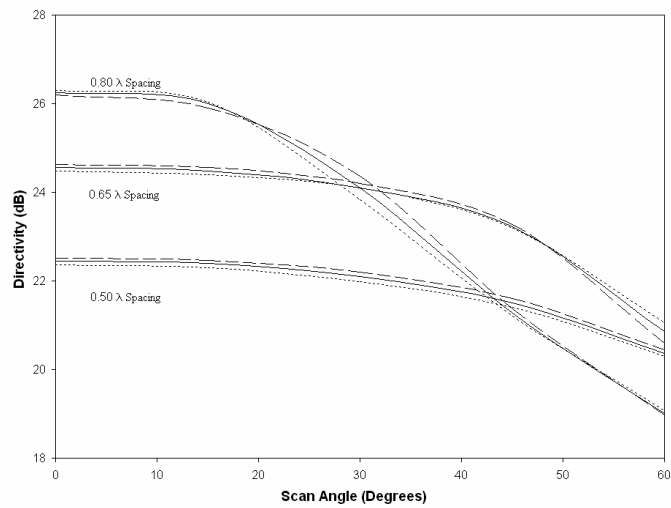


Figure 3. Directivities vs. scan angle.